(NASA-CR-169072) SEGREGATION DURING DIRECTIONAL MELTING AND ITS IMPLICATIONS ON SEEDED CRYSTAL GROWTH: A THEORETICAL ANALYSIS (Massachusetts Inst. of Tech.) 21 p HC A02/MF A01 CSCL 20L G3/76

N82-27157

Unclas 28962

SEGREGATION DURING DIRECTIONAL MELTING AND ITS IMPLICATIONS ON SEEDED CRYSTAL GROWTH: A THEORETICAL ANALYSIS

E. D. Bourret, J. J. Favier* and A. F. Witt

Department of Materials Science & Engineering
Massachusetts Institute of Technology
Cambridge, Massachusetts 02139

ABSTRACT

Directional melting of binary systems, as encountered during seeding in melt growth, is analyzed for concurrent compositional changes at the crystal-melt interface. It is shown that steady state conditions cannot normally be reached during seeding and that the growth interface temperature at the initial stages of seeded growth is a function of backmelt conditions. The theoretical treatment is numerically applied to $Hg_{1-x}Cd_xTe$ and Ga-doped Ge.

*Laboratoire d'Etudes de Solidification (DMG), C.E.N.G., Grenoble, France

1. INTRODUCTION

Directional melting, contrary to solidification, has been the subject of only very few studies. Woodruff and Forty (1) investigated melting and freezing of a Na-K alloy by in situ transmission UV microscopy; optical phenomena observed in their melting experiments have been interpreted as indicative for Na diffusion from the solid into the adjacent liquid phase. The directional melting studies by Verhoeven et al. (2) in Sn-Bi, carried out at a rate of 0.2 μm/sec, reportedly revealed a composition gradient region of 650 μm in the solid ahead of the receding interface. The establishment of such an extended gradient region (boundary layer) was found by them to conflict with theoretical prediction (1.3 μm) based on the application of their steady state segregation equation (3) for melting. It should be noted that the extended solute depleted region in their experiments was a two-phase region with liquid droplets appearing dispersed in the solid phase. They also report that no solute depletion region in the solid could be observed at higher melting rates (20 μm/sec). Verhoeven and Heimes (4) provided analytical solutions for initial melting transients with preceding solidification which consider diffusion in both the solid and liquid phases.

All seeded crystal growth from the melt involves as a first step a varying degree of backmelting of a crystal. This approach, generally successful in systems with small liquidus-solidus separation such as doped semiconductors, must, however, be expected to be problematic if binary or multicomponent systems with large liquidus-solidus separation ($Hg_{1-x}Cd_xTe$, $Pb_{1-x}Sn_xTe$, Ge-Si and the like) are involved. Any changes in composition that occur during melting at the crystal-melt interface are of importance since they control the growth interface temperature and its stability. Moreover, both parameters influence the system's behavior during equilibration (melting arrest) and may affect the

degree of crystalline and compositional perfection achievable during ensuing solidification. Seeded crystal growth, for exmple by the Bridgman and Czochralski techniques, involves directional melting under boundary and initial conditions which were not considered in the earlier treatments (4).

It is the purpose of this work to analyze the evolution of the solute concentrations, $C_S^*(t)$ and $C_L^*(t)$, at a crystal-melt interface and the related interface temperature during melting, with emphasis on the initial transient behavior. The analysis applies to binary systems in a configuration where a crystal of composition C_S in contact with a melt of composition C_L is directionally melted. The theoretical treatment is carried out in non-directional form; it is numerically applied to $Hg_{1-x}Cd_xTe$ and Ga-doped Ge to provide for comparative analysis of systems with small and large liquidus-solidus separation.

2. Theoretical Analysis of Solute Redistribution During Directional Melting

2.1 Definition of boundary conditions and mass transport relationships

The analysis for directional melting of binary solids is made with the following assumptions:

(a) the crystal-melt interface is planar; one-dimensional analysis;

(b) the interface displacement R is constant;

(c) the mass transports in the liquid and in the solid obey Fick's law;

(d) convection is neglected;

(e) the interface distribution coefficient k, taken to be identical with the equilibrium distribution coefficient, is a constant;

(f) the diffusion coefficients in the liquid (D_L) and in the solid (D_S) are constant;

(g) the initial length of the solid is larger than the characteristic length of diffusion;

(h) the initial compositions of the solid and contacting melt are in thermodynamic equilibrium ($C_S = kC_L$).

It is recognized that a constant D is not realized during melting since steep temperature and concentration gradients encountered across the crystal-melt interface must affect its magnitude. A detailed determination of the changing driving forces resulting from the existing gradients is complex because of their interdependence. Presently, the contributions of these driving forces are accounted for as an additional flux term, $J_F(z,t)$, which modifies Fick's second law as follows:

$$\nabla_t \cdot C(z,t) = -\nabla_z \cdot J(z,t)$$

with

$$J(z,t) = -D\nabla_z \cdot C(z,t) - \langle D_F \rangle \nabla_z \cdot C(z,t)$$

or

$$J(z,t) = -D_{eff}\nabla_z \cdot C(z,t)$$

where $D_{eff} = D + \langle D_F \rangle$ is defined as an "effective" coefficient of diffusion. The concept of D_{eff} has been used earlier (5) to account for the effect of convection. In this paper the notation D_S is used for D_{eff} in the solid and D_L for D_{eff} in the melt. With regard to assumption (e), it is customary in dilute binary systems such as doped semiconductors with small liquidus-solidus separation to take k to be independent of concentration. This approximation is in principle erroneous for systems with large liquidus-solidus separation.

The concentration dependence of k is known from the phase diagram and it could be added to the set of boundary conditions (providing that the displacement rate of the interface is constant - see Appendix). Since no general analytical treatment of the relationship between k(c,t) and R(t) is as yet available, R and k are taken to be constant.

2.2 Development of composition transients associated with directional melting

Making use of the preceding assumptions, Fick's second law, formulated for a coordinate system which moves with the interface according to the configuration shown in Fig. 1, assumes the form:

$$D_S \frac{\partial^2 C_S}{\partial z^2} + R \frac{\partial C_S}{\partial z} = \frac{\partial C_S}{\partial t} \qquad [1]$$

$$D_L \frac{\partial^2 C_L}{\partial z^2} + R \frac{\partial C_L}{\partial z} = \frac{\partial C_L}{\partial t} \qquad [2]$$

The initial and boundary conditions for equations [1] and [2] are:

$$t = 0 \qquad C_S = C_o \qquad z \varepsilon]0, +\infty] \qquad [3]$$

$$C_L = C_o/k \qquad z \varepsilon]0, -\infty] \qquad [4]$$

at the interface (z = 0):

$$C_S^* = k\, C_L^* \qquad \forall\, t \geq 0 \qquad [5]$$

Solute flux conservation through the interface yields:

$$D_S \left.\frac{\partial C_S}{\partial z}\right|_{z=0^+} + R\, C_S^* = D_L \left.\frac{\partial C_L}{\partial z}\right|_{z=0^-} + R\, C_L^* \qquad \forall\, t > 0 \qquad [6]$$

Using the change of scale:

$$\overline{C} = C - C_o \qquad [7]$$

Fig. 1

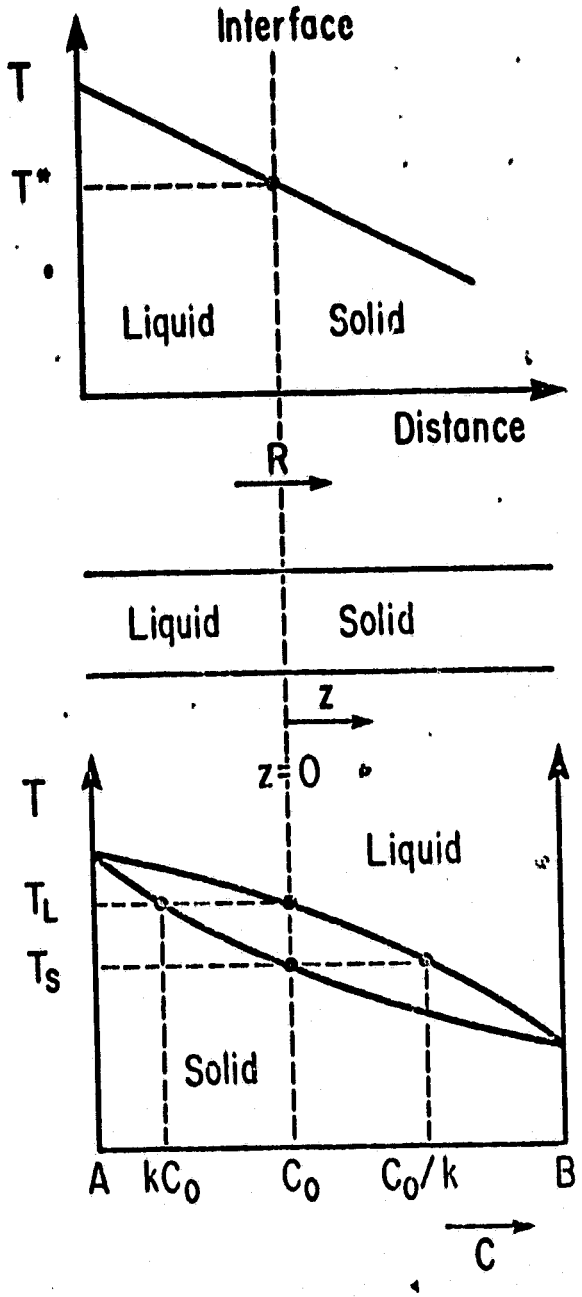

and the dimensionless variables:

$$y = \frac{Rz}{D_L} \quad [8] \qquad \tau = \frac{R^2 t}{D_L} \quad [9] \qquad \alpha = \frac{D_S}{D_L} \quad [10]$$

the system of eqs. [1] and [2] becomes:

$$\alpha \frac{\partial^2 \overline{C_S}}{\partial y^2} + \frac{\partial \overline{C_S}}{\partial y} = \frac{\partial \overline{C_S}}{\partial \tau} \quad [11]$$

$$\frac{\partial^2 \overline{C_L}}{\partial y^2} + \frac{\partial \overline{C_L}}{\partial y} = \frac{\partial \overline{C_L}}{\partial \tau} \quad [12]$$

with the corresponding initial and boundary conditions:

$$\tau = 0 \qquad \overline{C_S} = 0 \qquad y \in]0, +\infty] \quad [13]$$

$$\overline{C_L} = C_o\left(\frac{1}{k} - 1\right) \qquad y \in]0, -\infty] \quad [14]$$

at the interface (y = 0):

$$\overline{C_S^*} = k\overline{C_L^*} + C_o(k - 1) \qquad \forall\, \tau \geq 0 \quad [15]$$

$$\left.\frac{\partial \overline{C_S}}{\partial y}\right|_{y=0^+} + \overline{C_S^*} = \left.\frac{\partial \overline{C_L}}{\partial y}\right|_{y=0^-} + \overline{C_L^*} \,. \quad [16]$$

The set of equations [11-12] with the boundary conditions [14 to 16] and the initial conditions [13] can be solved by using the Laplace transforms:

$$\tilde{\gamma}_S = \int_0^\infty \overline{C_S}\, e^{-s\tau} d\tau \quad [17]$$

and

$$\tilde{\gamma}_L = \int_0^\infty \overline{C_L}\, e^{-s\tau} d\tau \quad [18]$$

yielding:

$$\alpha \frac{d^2\tilde{\gamma}_S}{dy^2} + \frac{d\tilde{\gamma}_S}{dy} - \delta\, \tilde{\gamma}_S = 0 \qquad [19]$$

$$\frac{d^2\tilde{\gamma}_L}{dy^2} + \frac{d\tilde{\gamma}_L}{dy} - \delta\, \tilde{\gamma}_L = -q \qquad [20]$$

with

$$q = C_o\left(\frac{1}{k} - 1\right) \qquad [21]$$

Taking the general solutions:

$$\tilde{\gamma}_S = A\, e^{-ay/\alpha} \qquad [22]$$

$$\tilde{\gamma}_L = B\, e^{-by} + \frac{q}{\delta} \qquad [23]$$

and using [13 to 16], one obtains:

$$\tilde{\gamma}_S = \frac{kq}{\delta} \frac{\exp\left(-\frac{1}{2} - \sqrt{\frac{1}{4} + \delta\alpha}\right)\frac{y}{\alpha}}{k - \frac{k}{2\alpha} - \frac{1}{2} - \frac{k}{\alpha^{3/2}}\sqrt{\frac{1}{4} + \delta\alpha} - \sqrt{\frac{1}{4} + \delta}} \qquad [24]$$

and

$$\tilde{\gamma}_L = \frac{q}{\delta}\left[1 + \frac{\exp\left(-\frac{1}{2} + \sqrt{\frac{1}{4} + \delta}\right)y}{k - \frac{k}{2\alpha} - \frac{1}{2} - \frac{k}{\alpha^{3/2}}\sqrt{\frac{1}{4} + \delta\alpha} - \sqrt{\frac{1}{4} + \delta}}\right] \qquad [25]$$

These relationships depend mainly on the two parameters k and $\alpha = D_S/D_L$. The inverse Laplace transforms are obtained in the general case by a numerical method. Analytical solutions will be given for particular values of α.

The inverse Laplace transform is made by approximating the integral:

$$\overline{C}(y,\tau) = \frac{1}{2\pi i}\int_{c-i\infty}^{c+i\infty} e^{\delta\tau}\tilde{\gamma}(\delta)d\delta \qquad [26]$$

by a trapezoidal rule using discrete values of the Laplace transform $\tilde{\gamma}(\delta)$ along the integration path $\delta = c + i\omega$. For this purpose the integral [26] is approximated by Fourier cosine series which are evaluated using the Fast Fourier transform algorithm. The numerical inversion of [24] gives $\overline{C_S}(y,\tau)$ for given values of α and k. Figure 2 is a plot of $\tau_{0.99}$, the time necessary to reach 99% of steady state as a function of k, for four different values of α obtained by the inversion of [24]. [The real time (t) is related to the dimensionless time τ through $t = D_L\tau/R^2$.]

At the hypothetical upper limit ($\alpha = 1$), the liquid and the solid behave symmetrically and a corresponding solution of [24] is given by:

$$\overline{C_S}(y,\tau) = \frac{C_o}{2}(1-k)\operatorname{erfc}\left(\frac{y}{2\sqrt{\tau}} - \frac{\sqrt{\tau}}{2}\right)\exp(-y) - \frac{C_o}{2}\operatorname{erfc}\left(\frac{y}{2\sqrt{\tau}} - \frac{\sqrt{\tau}}{2}\right) \qquad [27]$$

which reduces at the interface to:

$$\overline{C_S^*}(0,\tau) = C_o(k-1)\operatorname{erf}\frac{\sqrt{\tau}}{2} \qquad [28]$$

Equation [28] confirms the plotted data, 99% of steady state ($\operatorname{erf}\frac{\sqrt{\tau}}{2} = 0.99$) is reached for all values of $k \neq 1$, with $\tau = 13.4$. The corresponding curve on Fig. 2 is used as a reference line to determine the variation of $\tau_{0.99}$ with α for any given value of k.

Considering the special case of $\alpha \to 0$, the inversion of [24] yields:

$$\overline{C_S}(y,\tau) = \frac{C_o}{2}\left\{(1-k)\operatorname{erfc}\left(\frac{y}{2\sqrt{\tau}} - \frac{\sqrt{\tau}}{2}\right)\exp(-y) + \frac{1}{k}\operatorname{erfc}\left(\frac{y}{2\sqrt{\tau}} + \frac{\sqrt{\tau}}{2}\right)\right.$$
$$\left. - \left(\frac{2-k}{k}\right)\exp\left(\frac{2-k}{2k} - \frac{1}{2}\right)y\ \exp\left(\frac{1-k}{k^2}\tau\right)\operatorname{erfc}\left(\frac{y}{2\sqrt{\tau}} + \frac{2-k}{2k}\sqrt{\tau}\right)\right\} \qquad [29]$$

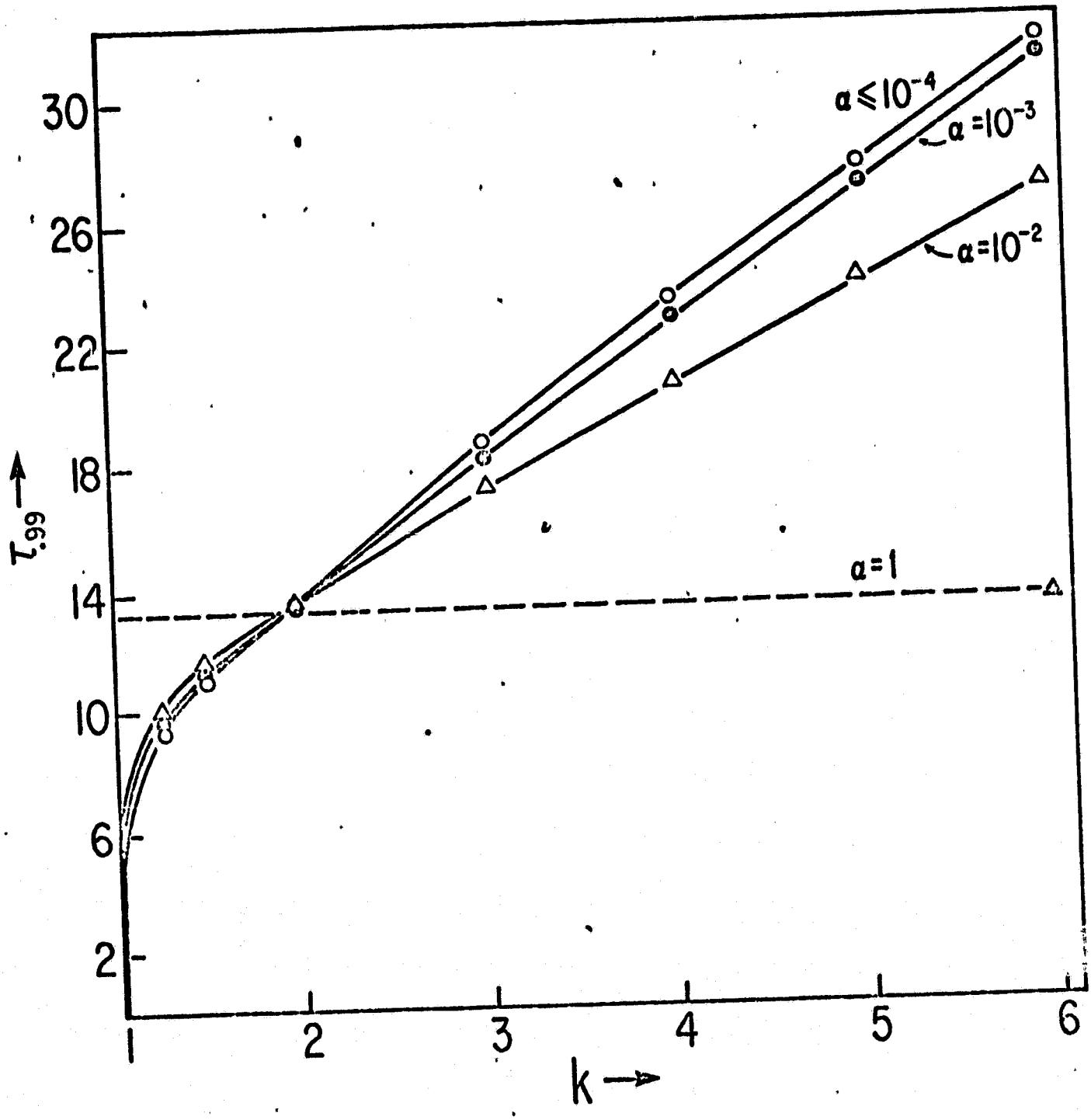

$$\overline{C_S}(0,\tau) = \frac{C_o}{2}\left((1-k)\operatorname{erfc}\left(\frac{-\sqrt{\tau}}{2}\right) + \frac{1}{k}\operatorname{erfc}\left(\frac{\sqrt{\tau}}{2}\right)\right.$$

$$\left. - \left(\frac{2-k}{k}\right)\exp\left(\frac{1-k}{k^2}\tau\right)\operatorname{erfc}\left(\frac{2-k}{2k}\tau\right)\right) \qquad [30]$$

2.3 Discussion of segregation analysis

The relationships [29] and [30] can be applied to solidification by using the transform S defined by $k \xrightarrow{S} 1/k$, $S \xrightarrow{S} L$, $L \xrightarrow{S} S$. It yields a solution which is identical with that given by Smith et al. (7) where D_S is considered negligibly small. Figure 2 shows that τ curves drawn for different values of α converge to equation [29] for $\alpha \leq 10^{-4}$. Generally accepted values for D_S and D_L in semiconductors lie in the range $10^{-10} - 10^{-8}$ cm^2/sec for D_S and $5 \times 10^{-4} - 10^{-5}$ cm^2/sec for D_L. Therefore the Smith et al. solution (or its equivalent for melting [29]) must be considered a good approximation. It should be pointed out, however, that as yet there are only limited data (of reasonable precision) for diffusion coefficients at melting point temperatures. While the uncertainty concerning the magnitude of D_L is not expected to have a noticeable effect on the value of α, D_S can be considerably larger than determined by extrapolation from lower temperatures. The temperature controlled increase in vacancy concentration, for example, will affect D_S and may thus have a significant effect on the value of α. The data show that already for $\alpha = 10^{-3}$ the Smith et al. approximation (or eq. [29]) no longer applies, and that for any given interface displacement rate, the compositional transients in the solid ($\tau_{0.99}$) (and in the liquid) increase with increasing α for $k < 2$ and decrease for $k > 2$.

2.4 Implications of segregation behavior on seeded crystal growth

It is of interest to consider the present analysis in terms of real time (t) behavior, i.e. to consider, for example, the specific effect of the rate of

directional melting (R) on the time required to reach steady state. For this purpose, it is convenient to analyze the behavior of specific systems. An arbitrary choice is $Hg_{1-x}Cd_xTe$ of the composition $x = 0.2$ ($C_o = 0.2$). Figure 3 presents the concentration of CdTe in the solid (HgCdTe) at the crystal-melt interface (C_S^*) as a function of τ for k_S and k_L. In real time (t), the CdTe concentration (C_S^*) is dependent on the rate of melting (R) which, in order to be meaningful, must satisfy the stability criteria (3). At the beginning of melting, the system is at equilibrium [$C_S(z,0) = C_o$, $C_L(z,0) = C_o/k$], and therefore under conditions of absolute stability. As melting proceeds, the interface stability is affected by out-diffusion and the subsequent formation of the boundary layer in the solid. Thus, while for $C_L(0,z) = C_o/k$ melting can be initiated at any rate, out-diffusion and interface breakdown must be anticipated if the rate exceeds a critical value. If the stability criterion is strictly applied to a steady state melting configuration, the G_S/R ratio required for stability is very high ($\simeq 10^8$°C/sec for $Hg_{0.8}Cd_{0.2}Te$). Such a high value is achieved by either a very high thermal gradient or a very slow rate of interface displacement. Making use of Fig. 3 and applying numerical values for HgCdTe, the present analysis shows that under neither condition will steady state be reached during seeding in Bridgman or Czochralski growth where the seed is back-melted for several millimeters only (see Table I); the crystal-melt interface temperature during melting must therefore be expected to lie somewhere between the solidus and the liquidus temperatures. Considering the back-melting of an ingot of $Hg_{0.8}Cd_{0.2}Te$ for half an hour at the rate of 3.7×10^{-2} μm/sec (the rate required for absolute stability at steady state if $G_S = 1000$°C/cm), the τ value at the end of back-melting (i.e. after half an hour) is 4×10^{-4} and, according to Fig. 3, the concentration in the solid (C_S^*) will be essentially unchanged at C_o and the interface temperature will remain at about T_S.

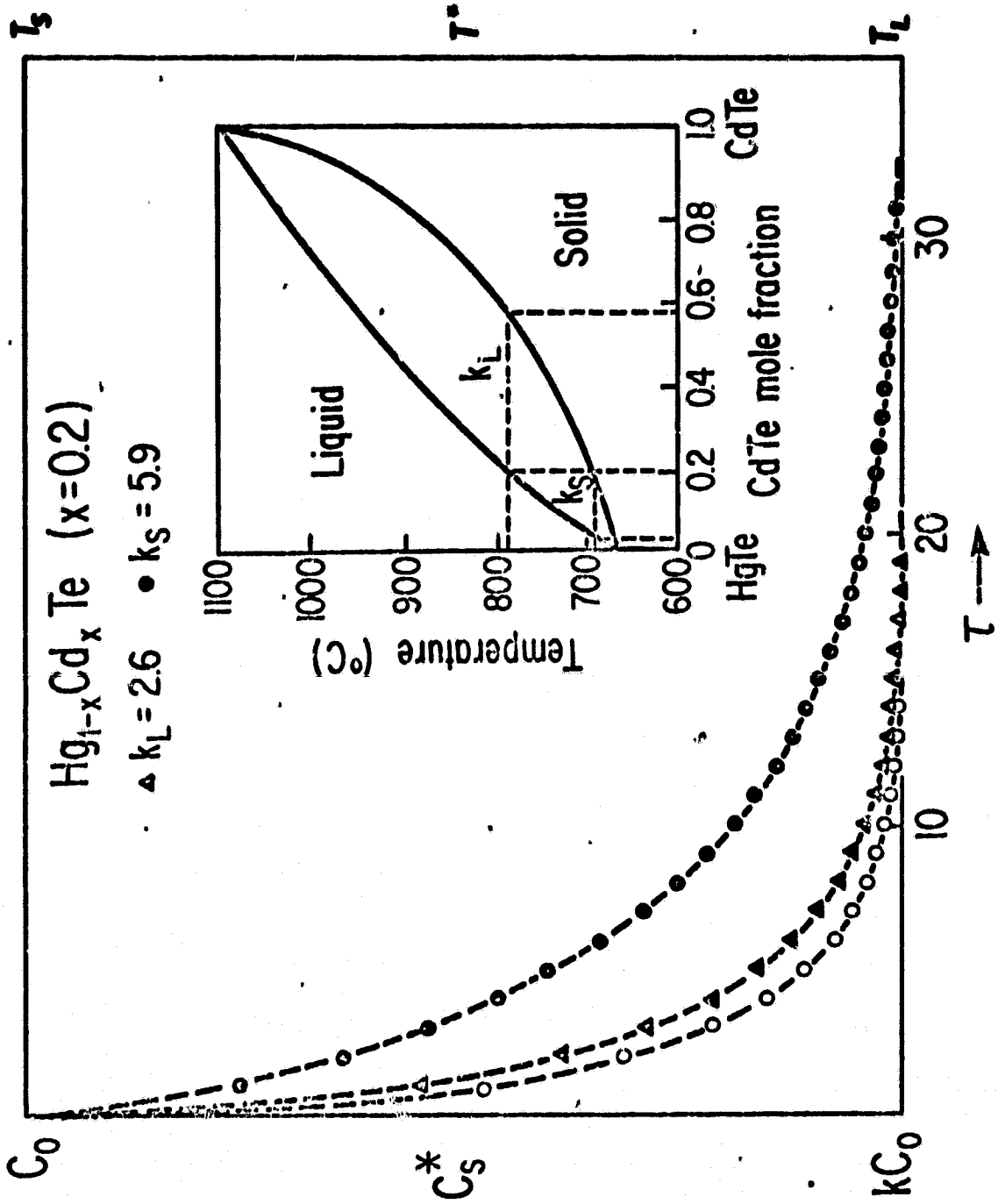

The dependence of the length of transient behavior on the magnitude of the liquidus-solidus separation can be demonstrated by comparing $Hg_{0.8}Cd_{0.2}Te$ with Ga-doped Ge where the liquidus-solidus separation is very small (less than 1°C). The τ curves of Ga-doped Ge are presented in Fig. 4. At the composition 10^{18} at/cm^3 of Ga, the G_S/R ratio assumes the value of 2.9×10^3 °C/sec (m_S = 0.366°C/%; $D_S = 10^{-8}$ cm^2/sec; k = 0.087). Since the Ga-doped Ge system has been extensively studied, the credibility of the data used for the different parameters is much higher than for HgCdTe. Table I shows that the length to be melted to reach steady state (z_m) in doped Ge is much smaller than in $Hg_{0.8}Cd_{0.2}Te$. The interface concentration in the solid under the conditions depicted in Table I can be calculated using the τ curves in Fig. 4. Assuming again that back-melting is to proceed for 0.5 hours at G_S = 10°C/cm and R = 34 μm/sec, we obtain a τ value of 99 which indicates that steady state has been reached and that the concentration in the solid at the interface, C_S^*, is kC_o. For this system, $\tau_{0.99}$ (steady state) is already reached after about 9 minutes. With continuing melting, the crystal-melt interface temperature changed from T_S to T_L, the liquidus temperature. It is noteworthy that for systems with a liquidus-solidus separation smaller than in $Hg_{0.8}Cd_{0.2}Te$ but larger than in very dilute systems, the temperature of the interface (T^*) at the end of back-melting is expected to be somewhere between T_S and T_L; its value, at a given time, can be calculated from appropriate τ curves. The interface temperature is related to the composition at the interface through the relation $T^* = T_m + m_t C_S^*$, where T_m is the melting temperature of the major constituent (for example, HgTe in $Hg_{0.8}Cd_{0.2}Te$) and m_t is the slope of the straight line joining T_m and the point on the solidus curve corresponding to the concentration C_S^* on the phase diagram. Therefore, the deviation of the interface temperature from the

Fig. 4

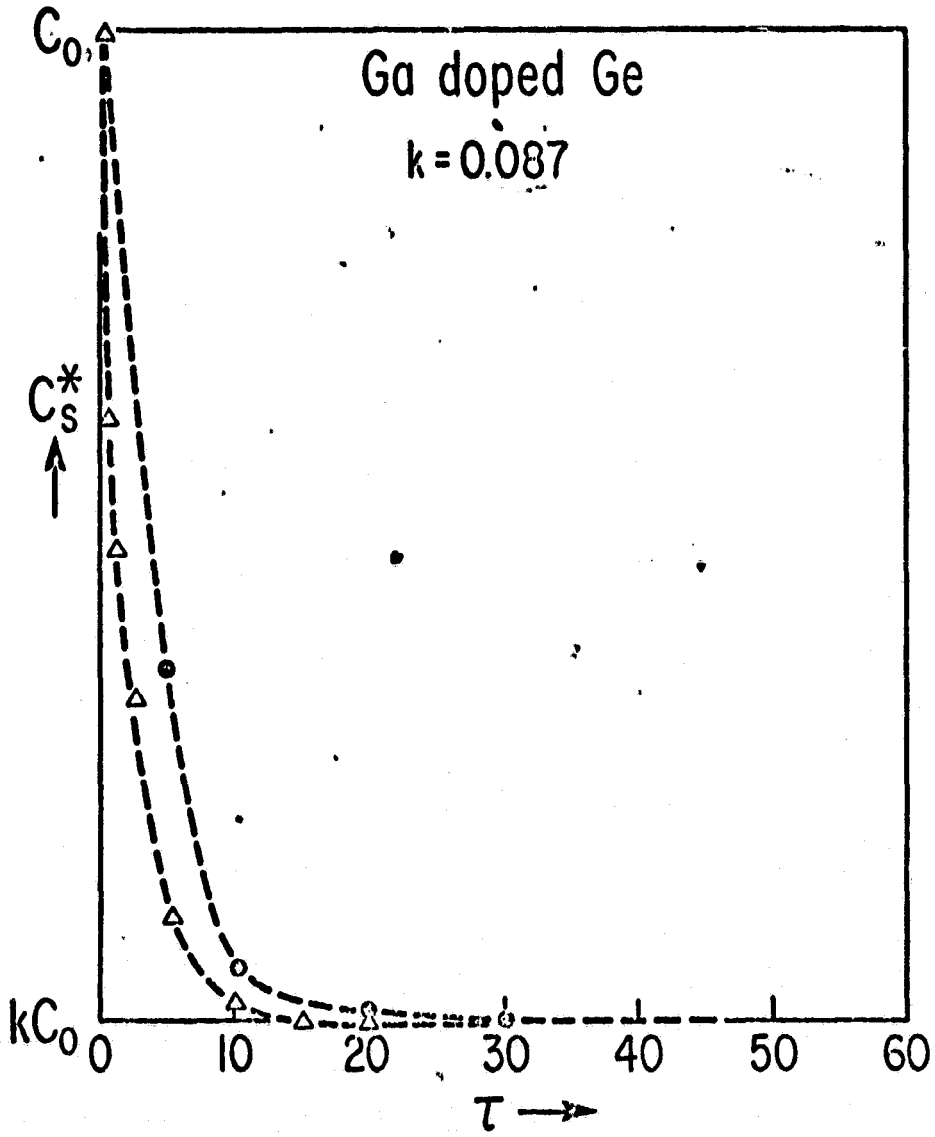

solidus temperature during transient melting ($\Delta T^* = T^* - T_S$) in non-dimensional notation is given by:

$$\Delta T^* = m_t C_S^* - m_{t=0} C_o \qquad [31]$$

As C_S^* approaches the value of kC_o, ΔT^* approaches a maximum value for which $T^* = T_L$.

The preceding analysis and conclusions apply to initial conditions whereby a (binary) solid is in thermodynamic equilibrium with the contacting melt ($C_S = kC_L$). This condition can in principle be realized during seeding in Czochralski and Bridgman-type growth. The analysis as such, however, is not applicable to configurations in which initially the entire charge is solid and seeded "re-growth" is accomplished by first directionally melting a fraction of the solid [configuration used during growth experiments in reduced gravity environment(8)]. Initial melting in this case cannot a priori be expected to take place at T_S. If the phase transformation is initiated under diffusionless conditions, melting will take place at $T_S < T_0 < T_L$, a temperature at which the solid and the liquid formed have equal free energies (9) but are at a different chemical potential. Maintaining this kinetically controlled metastable state will obviously be a function of the experimental conditions under which melting proceeds. Depending on the extent of diffusional adjustment of the phase boundary composition toward equilibrium, a transient in the crystal-melt interface temperature will be encountered. These transients to equilibrium for systems with $C_L \neq C_S/k$ are currently under investigation.

APPENDIX

As a consequence of segregation during transient melting or solidification the growth-interface temperature (T^*) is subject to change and the interface